Theoretical Insight into the Regioselective Ring-Expansions of Bicyclic Aziridinium Ions

Esma B. Boydas,[a] Gamze Tanriver,[a] Matthias D'hooghe,[b] Hyun-Joon Ha,[c] Veronique Van Speybroeck,[d] Saron Catak*[a,d]

[a]*Bogazici University, Department of Chemistry, Bebek 34342 Istanbul, Turkey*
[b]*Department of Sustainable Organic Chemistry and Technology, Faculty of Bioscience Engineering, Ghent University, Coupure Links 653, 9000 Ghent, Belgium*
[c]*Department of Chemistry, Hankuk University of Foreign Studies, Yongin, 17035, Korea*
[d]*Center for Molecular Modeling, Ghent University, Technologiepark 903, 9052 Zwijnaarde, Belgium*

Corresponding author: saron.catak@boun.edu.tr

ABSTRACT

Transient bicyclic aziridinium ions are known to undergo ring-expansion reactions paving the way to functionalized nitrogen-containing heterocycles. In this study, the regioselectivity observed in the ring-expansion reactions of 1-azoniabicyclo[n.1.0]alkanes is investigated from a computational viewpoint, to study the ring-expansion pathways of two bicyclic systems with different ring sizes. Moreover, several nucleophiles leading to different experimental results were investigated. The effect of solvation was taken into account with both explicit and implicit solvent models. The theoretical rationalization provides valuable insight into the observed regioselectivity and may be used as a predictive tool in future studies.

INTRODUCTION

There is a wide interest in aziridines due to their outstanding synthetic utilities as end-products and particularly as intermediates.[1,2] Release of ring strain in aziridines serves as a strong driving force in their ring-opening reactions, giving rise to a broad variety of functionalized nitrogen-containing target compounds.[3–5] Aziridine ring-opening reactions are mostly governed by the substituents on the ring nitrogen atom.[6,7] If the aziridine ring is endowed with an electron-withdrawing substituent at the ring nitrogen, it is classified as an "activated-aziridine".[8–11] Conversely, introduction of an electron-donating (alkyl) substituent at nitrogen results in a more inert aziridine ring, which is often referred to as a "non-activated aziridine" **(Scheme 1a)**[12–15] that requires activation with a proper electrophile, in order to undergo ring-opening **(Scheme 1b)**.[16] For example, *N*-alkylation of non-activated aziridines provides reactive aziridinium ions prone to undergo ring opening. Although such activated aziridinium ion intermediates have not been easily isolated –only a few examples of isolated (monocyclic) aziridinium salts have been reported[17]– their formation has usually been detected spectroscopically.[18,19]

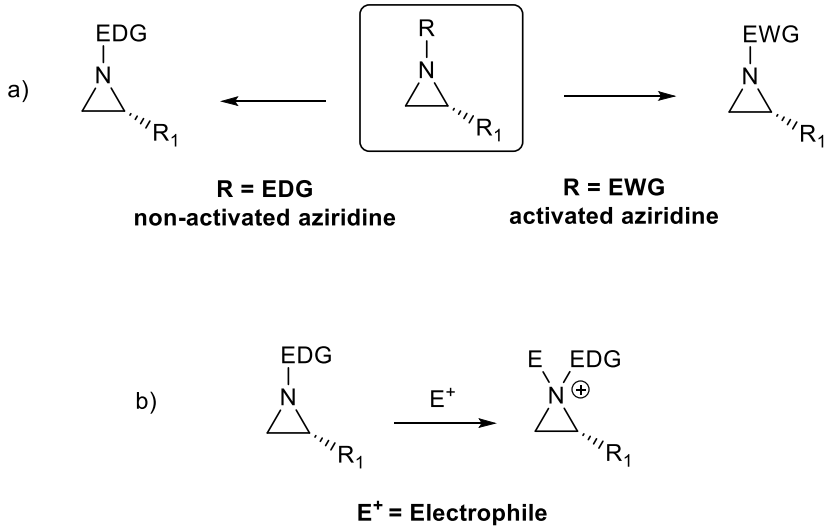

Scheme 1. a) Activated versus non-activated aziridines, b) activation of non-activated aziridines.

Monocyclic aziridinium ions, generated through *N*-alkylation with an external alkyl halide, could undergo ring-opening reactions with a proper nucleophile, to afford either α-branched amines *via* attack on the unsubstituted carbon or β-branched amines through attack on the more hindered carbon, as shown in **Scheme 2a**.[20,21]

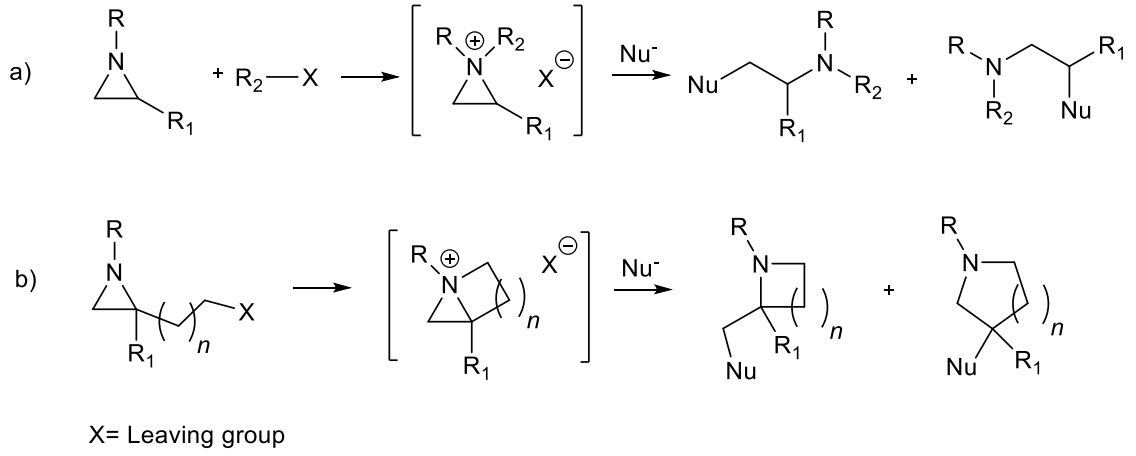

Scheme 2. Schematic representation of a) monocyclic and b) bicyclic aziridinium ion formation and their ring-opening reactions by nucleophiles.

In addition to monocyclic structures, bicyclic aziridinium ions can be generated in an intramolecular S_N2 fashion, from which ring-opening reactions would result in ring-expansions and lead to azaheterocyclic products,[22,23] as shown in **Scheme 2b**. Several studies reporting on the formation of bicyclic aziridinium moieties and their synthetic utilities are available.[15,24,25] The ring-expansion routes of bicyclic aziridinium ions mainly depend on their ring-size, nature of the aziridinium substituents and the identity of the nucleophile, which all contribute to determine the kinetic and thermodynamic properties of the reaction.

Recently, the formation of 1-azoniabicyclo[3.1.0]hexane tosylates **1** and their ring-expansion upon treatment with various nucleophiles in acetonitrile has been investigated by Ha and coworkers.[25]

This ring-expansion, as shown in **Scheme 3**, resulted in either piperidines **3** or pyrrolidines **4**, depending on the site of nucleophile attack. While ring-opening at the hindered aziridinium carbon, *via* **path i** affords piperidines **3**, attack on the unhindered carbon (through **path ii**) leads to pyrrolidines **4**. In Ha's work,[25] **(Scheme 3)** the cyanide nucleophile was shown to induce an attack on the less hindered carbon and exclusively yield pyrrolidines **4**, whereas chloride preferred the more hindered path and led to piperidines **3** as seen in **Table 1**.

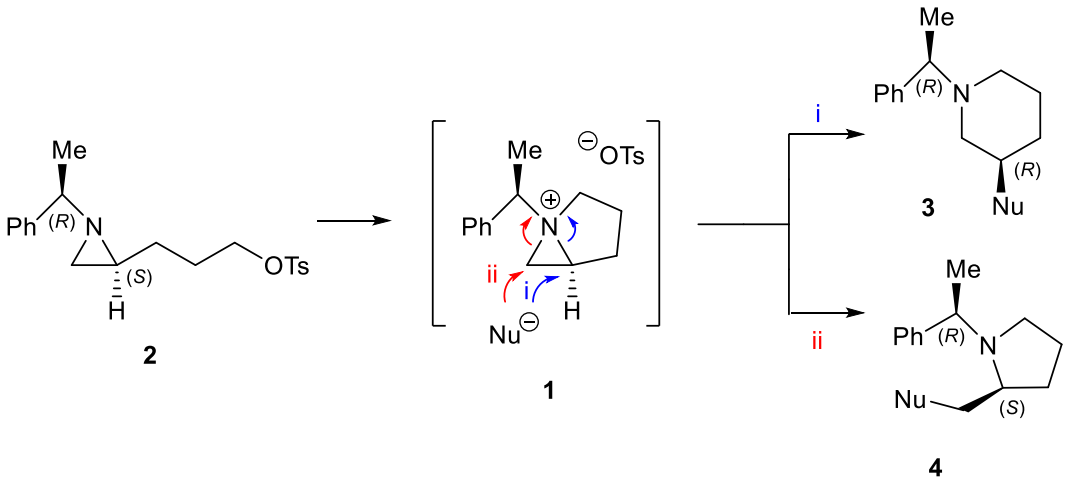

Scheme 3. The formation of 1-azoniabicyclo[3.1.0]hexane tosylates **1** and its corresponding ring expansion reaction by a nucleophile.[25]

More recently, the synthesis of 1-azoniabicyclo[4.1.0]heptane tosylates **5** and their ring-expansion products were proposed by Choi *et al*.[26] The subsequent ring-expansion reactions, conducted with different nucleophiles, resulted in either azepanes **7** by way of the more-hindered **path i**, or piperidines **8** by following **path ii**, as depicted in **Scheme 4**. Once again, cyanide was shown to attack the less hindered position, and mainly gave rise to piperidines **8** with **8:92** ratio (**Table 1**). There seems to be less of a distinction between the two routes for azide and amine attacks to aziridinium ion **5**, with product ratios of **59:41** and **65:35**, respectively, slightly in favor of the more hindered pathway leading to azepane **7** (**Table 1**).

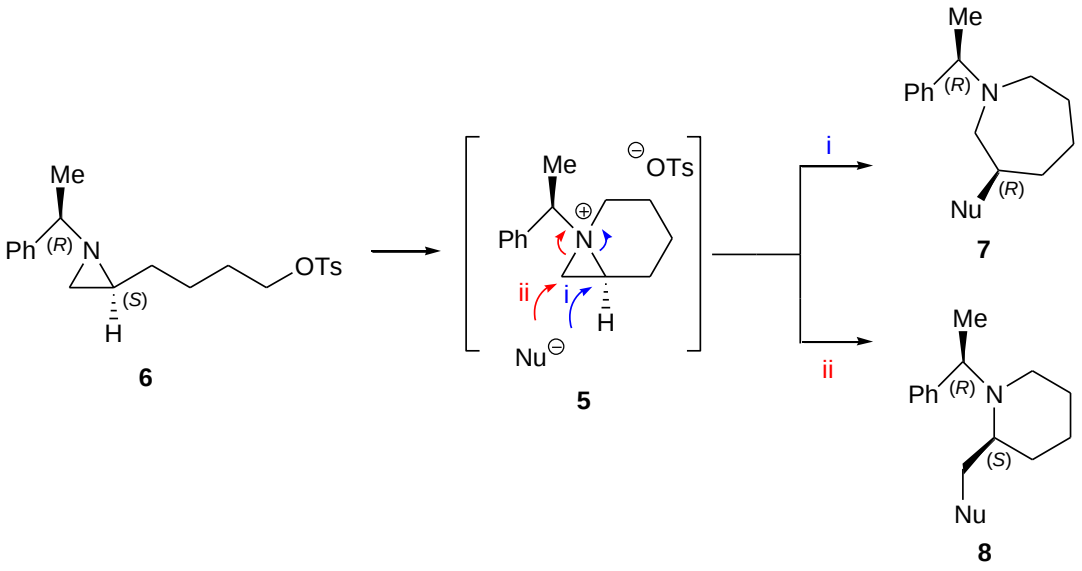

Scheme 4. The formation of 1-azoniabicyclo[4.1.0]heptane tosylate **5** and its corresponding ring expansion reaction by a nucleophile.

Table 1. Ring-expansion reactions of 1-azoniabicyclo[3.1.0]hexane tosylates **1**[25] and 1-azoniabicyclo[4.1.0]heptane tosylates **5**[26] with different nucleophiles in CH_3CN.

Nucleophile	Substrate	T [°C]	Yield (%)	**3/4** ratio	**7/8** ratio
nBu_4N^+**CN**$^-$	aziridinium **1**	25	89	0:100	-
Na**N**$_3$	aziridinium **1**	25	89	36:64	-
Ts**Cl**	aziridinium **1**	25	88	100:0	-
Na**CN**	aziridinium **5**	25	92	-	8:92
Na**N**$_3$	aziridinium **5**	25	92	-	59:41
Bn**NH**$_2$	aziridinium **5**	25	87	-	65:35

As seen from the product ratios in the reactions mentioned above, the factors governing the regioselectivity in ring-expansion of 1-azoniabicyclo[n.1.0]alkanes are yet unclear. There are many elements that contribute to the selectivity, such as the effect of solvent, the nature of the nucleophiles and electrophiles.[27] The present study aims to focus on these two recent examples, involving the formation and interception of 1-azoniabicyclo[3.1.0]hexane tosylates **1** and 1-

azoniabicyclo[4.1.0]heptane tosylates **5**, and to computationally explore the two competing reaction routes in an effort to elucidate the underlying elements that determine the preferred path in the ring expansions of bicyclic aziridiniums and lead to the experimental product distributions. Both aziridinium ions **1** and **5** bear the same *N*-substituent, allowing for a clear comparison of the effect of the ring size and the nature of the nucleophile.

The theoretical study of regioselectivity in complex reaction media as studied herein is quite challenging as recently reviewed by Houk and coworkers.[28] In-depth understanding of the transition state structures and accurate assessment of their energies is of utmost importance to make a distinction between the various competitive routes in mechanistic studies. Thus, the energy differences between the competing pathways for both 1-azoniabicyclo[n.1.0]alkane systems under study herein are of major interest and a proper modeling approach is pertinent in attaining reliable results and assessing the factors influencing the experimental results. The ring-expansion of 1-azoniabicyclo[3.1.0]hexane tosylates **1** has previously been analyzed by some of the authors in a joint experimental/computational study.[25] Herein, it will be re-visited, to account for dispersion interactions, which are well-known to significantly affect the outcome of organic reactions.[29–31] The aim is to aid the experimental strategy by shedding light on the factors affecting the regioselectivity in ring-expansions of bicyclic aziridiniums. Moreover, the ultimate goal is to establish a computational methodology able to predict the outcome of future studies on ring-expansions of these ions.

COMPUTATIONAL METHODOLOGY

To gain insight into the regioselective preference of different nucleophiles, towards the ring opening of 1-azoniabicyclo[3.1.0]hexane tosylates **1** and 1-azoniabicyclo[4.1.0]heptane tosylates

5, a thorough Density Functional Theory (DFT) study was performed. All reactants, transition states (TS) and products were optimized at the B3LYP[32] and M06-2X[33] level of theory utilizing the 6-31+G(d,p) and 6-31++G(d,p) basis sets. Conformational analysis was performed on all reactants, transition states and products in an effort to identify the most plausible conformers. Semi-empirical dispersion correction scheme DFT-D,[34,35] developed by Grimme, was used to account for dispersive and non-covalent interactions, as an add-on term to B3LYP energies, allowing for a comparison between M06-2X and B3LYP-D performance. Energy refinements were performed at MPW1K[36] and BMK[37] levels of theory, and 6-31+G(d,p) basis set. These functionals were specifically designed for predicting accurate barrier heights and kinetics.

All calculations were carried out with the Gaussian 09 software package.[38] Free energies were reported in kJ/mol at 1 atm and 298 K. Normal mode analysis was performed to identify the nature of the ground state and transition state structures. Furthermore, Intrinsic Reaction Coordinate (IRC)[39,40] calculations were used to verify the transition state geometries.

It has been shown that solvent effects cannot be neglected in the regioselective ring opening of aziridinium ions.[14,41,42] Hence, the possible pathways under study were modeled with several different levels of solvation. The simplest method of taking into account the solvent environment consists of using a continuum model, where the solute is placed in a continuous medium characterized by a dielectric constant.[43,44] Two well-known implicit solvation methods based on Polarizable Continuum Model (PCM), namely IEFPCM and CPCM, were used.[45,46] PCM models surely provide a better environment than gas phase calculations, however, they still are not able to take into account possible explicit interactions with solvent molecules. In addition to the implicit solvent approach, a discrete solvent model (also called the 'supermolecule' approach or

microsolvation)[27,47–51] was used to solvate the bicyclic aziridinium ions and the attacking nucleophiles in their corresponding transition states. The number of explicit solvent molecules was determined by the value at which the coordination solvation energy converged and was incorporated from a previous study on a similar system.[25] To also elucidate potential long-range interactions, the systems containing two explicit solvent (acetonitrile) molecules, were additionally placed in a dielectric continuum in an approach known as a mixed implicit/explicit model.[51–53]

In an effort to further understand the regioselectivity in the ring-expansion reactions of bicyclic aziridinium ions, the Distortion-Interaction Model also known as the Activation-Strain Model (ASM) was used.[54–56] The ASM model is very proficient in differentiating between the favorable interactions as well as the unfavorable distortions occurring in the transition state structure.[57,58] This model partitions the electronic activation energy $\Delta E^{\ddagger}$ into distortion energy ($\Delta E_{dist}^{\ddagger}$) and interaction energy ($\Delta E_{int}^{\ddagger}$) **(Scheme 5)**. Distortion energy represents the strain caused by deformation of the reactants in the course of transition state and is determined by the rigidity of the reactants. If the reaction coordinate entails a high reorganization within/among the reactants, distortion energy would be high. On the other hand, interaction energy stems from a stabilizing interaction between reactants, and is affiliated with how well reactants are oriented towards each other. In most cases, $\Delta E_{int}^{\ddagger}$ is negative and stabilizing, and $\Delta E_{dist}^{\ddagger}$ is positive and destabilizing.[27,47,48,55,59,60]

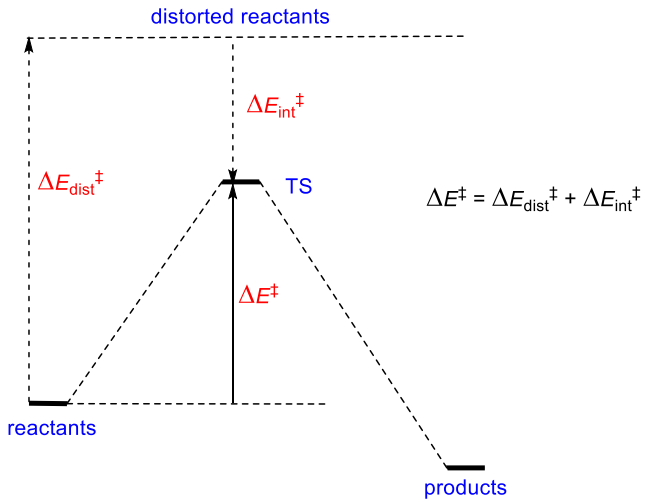

Scheme 5. Schematic illustration of the distortion-interaction model.[54–56]

RESULTS AND DISCUSSION

In an effort to elucidate the factors governing the selectivity in ring-expansion reactions of 1-azoniabicyclo[n.1.0]alkane systems, the two possible routes in **Schemes 3** and **4** were computationally explored with several different nucleophiles, as summarized in **Table 1**. In particular, the interaction of CN^-, N_3^-, and Cl^- with aziridinium ion **1** was investigated, as well as the reaction of CN^-, N_3^-, and NH_2^- for the ring-expansion reactions of aziridinium ion **5**. The hybrid GGA functional B3LYP was used for optimizations, as well as the meta-GGA M06-2X, which is known to perform well with non-covalent interactions and produce accurate thermochemical data.[33,61]

Transition state structures for all nucleophiles are shown in **Figure 1** for both systems. Explicit acetonitrile molecules were placed in a consistent manner around the attack sites; the positive dipole of solvent molecules interacts with nucleophiles at a distance of 2.0–3.0 Å. Counter ions of the nucleophiles and the tosylate ion were not included in the calculations, since they are unlikely

to have a close association with the aziridinium ion in the presence of such a high-dielectric solvent. It is important to note that, while nucleophile attack distances are similar for both pathways in the case of aziridinium **1**, they significantly differ for aziridinium **5** indicating the importance of ring size in nucleophile-induced ring expansions of bicyclic aziridinium ions. Moreover, taking into account the C-N distances in the aziridinium ions, the extent of reaction is shown to be somewhat similar for pathways in the case of aziridinium ion **1**. However, in the aziridinium ion **5** case, the transition state leading to the unhindered pathway (**path ii**) is clearly much more reactant-like (see shorter aziridinium C-N distances) than their **path i** counterparts, which have much larger C-N distances indicating a later TS. A more elaborate analysis of the critical distances will be given in the following section.

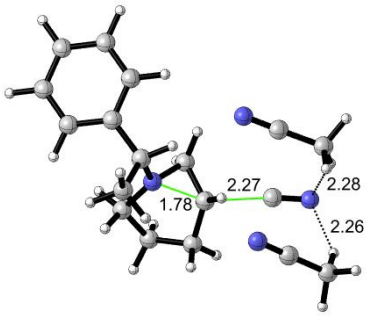

1-CN-i

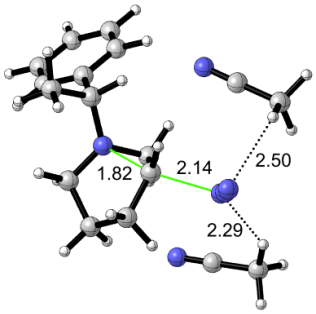

1-N$_3$-i

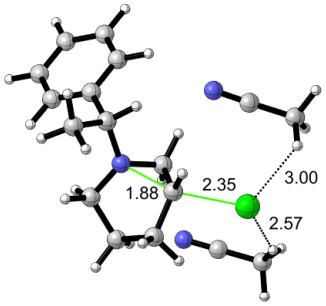

1-Cl-i

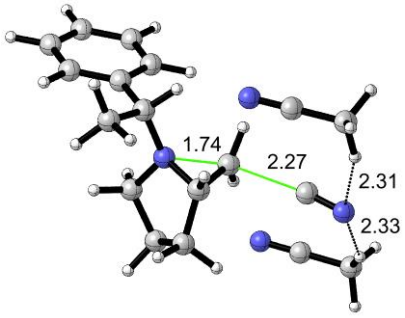

1-CN-ii

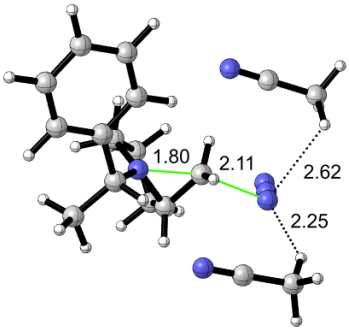

1-N$_3$-ii

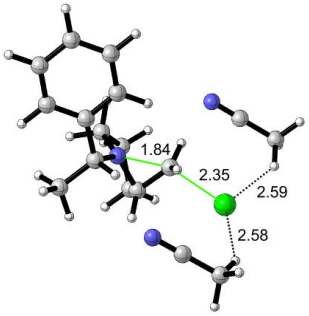

1-Cl-ii

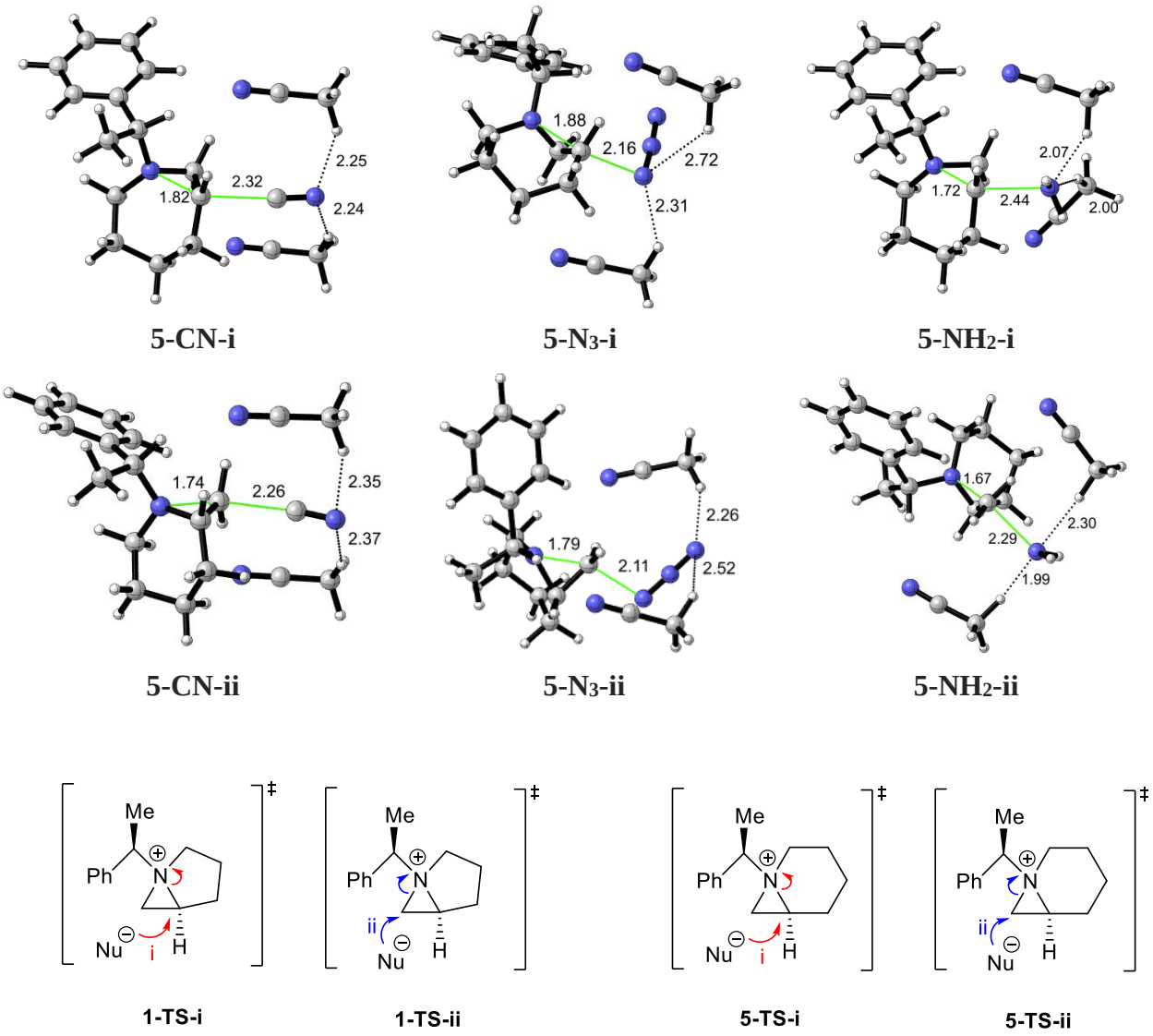

Figure 1. Transition state structures of **path i** (hindered) and **path ii** (unhindered) for the ring opening of bicyclic aziridinium ions **1**[25] (top) and **5**[26] (bottom) with different nucleophiles. (M06-2X/6-31+G(d,p); two explicit acetonitrile molecules; critical distances in Å)

Bond Elongation Analysis

The reaction mechanism has been further investigated by calculating the variation of critical distances along different routes for 1-azoniabicyclo[n.1.0]alkanes **1** and **5**. Bond elongation percentages were calculated with respect to the nitrogen-carbon distances in bicyclic aziridinium ions **1** and **5**, as illustrated in **Table 2**. Several different methods of solvation were used in the

optimization of the transition states. Both implicitly solvated (IEFPCM), and explicitly solvated transition states are comparatively examined in this section.

As mentioned earlier, steric effects and the nature of the nucleophile determine the attack distance. The hindered aziridinium carbon atom (**C2**) is not easily approached by a nucleophile and the critical distances are expected to be longer for **path i**; this effect is more pronounced in the case of aziridinium ion **5,** due to the larger ring size. For both aziridinium ions **1** and **5**, bond elongation percentages for the unhindered aziridinium carbon P(N-C3) are smaller than those for P(N-C2), indicating that in all cases regardless of ring size and nucleophile identity the hindered attack is always more distorting than its unhindered counterpart. When solvation effects are considered, implicitly solvated transition states often have higher bond elongation percentages than their explicit counterparts indicating earlier TS's in the latter.

Table 2. Transition state critical distances (Å) and bond elongation percentages of **path i** (hindered) and **path ii** (unhindered) for bicyclic aziridinium ions **1** and **5**.[a-e]

M06-2X/6-31+G(d,p), 298 K and 1 atm.

			path i (*hindered)*			**path ii** *(unhindered)*		
		Azirid.	*d*(Nu-C2)	*d*(N-C2)	P(N-C2)[c-e] (%)	*d*(Nu-C3)	*d*(N-C3)	P(N-C3)[c-e] (%)
CN^-	implicit	**1**	2.23	1.83	22.8	2.22	1.79	20.9
	explicit	**1**	2.27	1.78	19.5	2.27	1.74	17.6
N_3^-	implicit	**1**	2.11	1.86	24.8	2.08	1.82	23.0
	explicit	**1**	2.14	1.82	22.1	2.11	1.8	21.6
Cl^-	implicit	**1**	2.32	1.93	29.5	2.30	1.9	28.4
	explicit	**1**	2.35	1.88	26.2	2.35	1.84	24.3
CN^-	implicit	**5**	2.27	1.86	24.0	2.21	1.79	20.9

N_3^-	explicit	**5**	2.32	1.82	21.3	2.26	1.74	17.6
	implicit	**5**	2.13	1.90	26.7	2.08	1.83	23.6
NH_2	explicit	**5**	2.16	1.88	25.3	2.11	1.79	20.9
	implicit	**5**	2.39	1.74	16.0	2.36	1.66	12.2
	explicit	**5**	2.44	1.72	14.7	2.29	1.67	12.8

[a] Implicit solvent model: IEFPCM in acetonitrile (ε =35.688).
[b] Explicit solvent model: Two explicit acetonitrile molecules.
[c] Bond elongation percentages P(N-C) (%) = $(d_{TS} - d_{reactant})/(d_{reactant})$x100.
[d] *d*(N-C2) = 1.49 Å, *d*(N-C3) =1.48 Å from bicyclic aziridinium ion **1**.
[e] *d*(N-C2) = 1.50 Å, *d*(N-C3) = 1.48 Å from bicyclic aziridinium ion **5**.

In the case of ring-expansion of bicyclic aziridinium ion **1** with explicit solvent model, the critical distances between the incoming nucleophile and the S_N2 carbon, are 2.27 and 2.35 Å for cyanide and chloride, respectively, for both paths **i** and **ii**. However, it is important to note that the extent to which the ring has opened in the chloride case (1.88 and 1.84 Å carbon-nitrogen distances for explicitly solvated **path i** and **ii**, respectively) is indicative of a late and more 'product-like' transition state, which tend to lead to the thermodynamic product. Moreover, cyanide is shown to attack the aziridinium ring at shorter distances, leading to earlier more 'reactant-like' transition state structures that typically lead to the kinetic product. For both bicyclic systems, azide is shown to attack at closer distances, moreover, with its higher bond-elongation values, a more "product-like" transition state is depicted. NH_2^- induces the lowest elongation along the nitrogen-carbon bond, by around 12-16% for each aziridinium carbon. This is a clear indication of the very early nature of the TS and the high reactivity of the nucleophile. In an effort to pinpoint the consequences of the differential critical distances, the distortion-interaction model was utilized in the next sections.

Energetic Analysis

The differences in Gibbs free energy of activation (**ΔΔ*G*‡**) between **paths i** and **ii**, for the explicitly solvated ring-expansion of bicyclic aziridinium ions **1** and **5** were tabulated in **Table 3**. Energy refinements with IEFPCM were performed on the explicitly solvated reaction systems shown in **Figure 1**, in order to assess the effect of a mixed implicit/explicit model. The results of the mixed solvation model were compared with explicitly solvated systems *in vacuo* as well as the implicitly solvated systems (**Table 3**). No significant difference in energetic trends was observed by the incorporation of the dielectric continuum on the explicitly solvated system. Henceforth, the study will use explicit-implicit models and exclude mixed solvation models.

Table 3. Differences of Gibbs free energies of activation (**ΔΔ*G*‡**) for the ring-expansion of 1-azoniabicyclo[n.1.0]alkane **1** and **5** with different nucleophiles.[a-d]

M06-2X/6-31+G(d,p) energies in kJ/mol at 298 K and 1 atm.

Nu	Aziridinium	ΔΔ*G*‡			
		Explicit[a]		Explicit/Implicit[b,c]	
		path i *(hindered)*	**path ii** *(unhindered)*	**path i** *(hindered)*	**path ii** *(unhindered)*
CN^-	**1**	13.7	0.0	8.7	0.0
N_3^-	**1**	7.9	0.0	7.7	0.0
Cl^-	**1**	10.3	0.0	13.2	0.0
CN^-	**5**	11.4	0.0	13.9	0.0
N_3^-	**5**	2.4	0.0	6.4	0.0
NH_2^-	**5**	10.0	0.0	8.3	0.0

[a] Two explicit acetonitrile molecules.
[b] Two explicit acetonitrile molecules.
[c] Energy refinement with IEFPCM in acetonitrile (ε =35.688).
[d] All energies relative to the pre-reactive complex (PRC) of path **ii**.

When differences in barriers for the competing pathways are considered (**Table 3)**, the unhindered route (**path ii**) is shown to be the kinetic path for both aziridinium **1** and **5**, as expected. This data would suggest that aziridinium ions **5** would yield piperidines **8** with all nucleophiles. Similarly, ring-opening of aziridinium ions **1** with all nucleophiles would result in the formation of pyrollidines **4**. However, this is not the experimental outcome and this data alone is not conclusive and only points toward the kinetically favored pathway, which is the unhindered route (**path ii**). In order to rationalize the experimental outcome several factors, such as product stabilities, relative barrier heights for the reverse reactions, thermodynamic equilibration as well as feasibility of the reactions under experimental conditions, need to be considered for each case. A more detailed discussion of the free energy profiles is given in the following section.

Gibbs free energies of activation ($\Delta G^{\ddagger}$) and reaction (ΔG_{rxn}) for the ring opening of both bicyclic aziridinium ions **1** and **5** are reported in **Table 4**. Energy refinements with Grimme's dispersion correction scheme were implemented on B3LYP optimizations. In addition, optimizations with the dispersion-corrected GGA M06-2X are reported. Computed data in **Table 4** reveals that activation barriers are consistently higher with the M06-2X functional for each system, possibly due to the extra stabilization of the reactants with dispersion effects. Moreover, barrier heights for implicitly solvated systems (IEFPCM, **Table 4** and CPCM results in **Table S1**) are higher than their explicit counterparts, since the reference point in these calculations are separate reactants as opposed to pre-reactive complexes, in the latter explicitly solvated systems. Furthermore, implicit solvent models show almost identical results, indicating that the high-dielectric solvent, acetonitrile, is sufficiently mimicked by implicit models. It should be noted that due to their reference state (separate reactants), relative barriers attained through PCM calculations are less prone to conformational bias and as such, IEFPCM results will be used in the remainder of the discussion.

Table 4. Gibbs free energies of activation ($\Delta G^{\ddagger}$) and reaction (ΔG_{rxn}) [kJ/mol] for the ring opening of bicyclic aziridinium ions **1** and **5** with different nucleophiles.

			B3LYP-D/6-31++G(d,p)[e]				M06-2X/6-31+G(d,p)				
			Path **i**	Path **ii**	Path **i**	Path **ii**	Path **i**	Path **ii**	Path **i**	Path **ii**	
		Nu	$\Delta G^{\ddagger}$		ΔG_{rxn}		$\Delta G^{\ddagger}$		ΔG_{rxn}		**Exp**[f]
Explicit Solvent [a,b]	**1**	**CN**	29.9	19.7	-211.5	-204.8	44.0	30.3	-204.2	-201.1	0:100
	1	**N_3**	31.8	28.5	-123.4	-105.4	50.9	43.0	-127.0	-112.4	36:64
	1	**Cl**	27.9	21.8	-68.5	-50.7	51.3	41.1	-63.5	-46.5	100:0
	5	**CN**	32.7	23.8	-180.7	-193.3	49.6	38.2	-178.7	-196.8	8:92
	5	**N_3**	28.2	27.1	-92.0	-109.6	66.6	64.2	-79.2	-81.4	59:41
	5	**NH_2**	40.1	28.8	-250.1	-253.3	26.6	16.6	-286.4	-292.1	65:35
Implicit solvent **(IEFPCM)** [c,d]	**1**	**CN**	70.0	61.6	-151.4	-140.0	**89.6**	**77.4**	-150.2	-139.4	0:100
	1	**N_3**	59.5	58.4	-75.9	-57.0	**82.0**	**78.6**	-83.0	-63.7	36:64
	1	**Cl**	75.2	69.5	-1.5	15.0	**96.7**	**90.8**	-7.7	11.4	100:0
	5	**CN**	67.9	63.8	-127.0	-139.2	**90.5**	**78.2**	-124.3	-136.8	8:92
	5	**N_3**	59.1	59.8	-54.0	-57.6	**87.3**	**78.2**	-61.6	-62.8	59:41
	5	**NH_2**	38.2	31.0	-239.5	-242.0	**54.9**	**43.1**	-249.9	-252.5	65:35

[a] All energies relative to the pre-reactive complex (PRC) of path **ii**.

[b] Optimizations with two explicit acetonitrile molecules in gas phase.

[c] All energies relative to the separate reactants.

[d] Optimizations with IEFPCM in acetonitrile (ε =35.688).

[e] Energy refinement with DFT-D dispersion correction.

[f] Experimental results **3:4** for aziridinium **1**, **7:8** for aziridinium **5.**

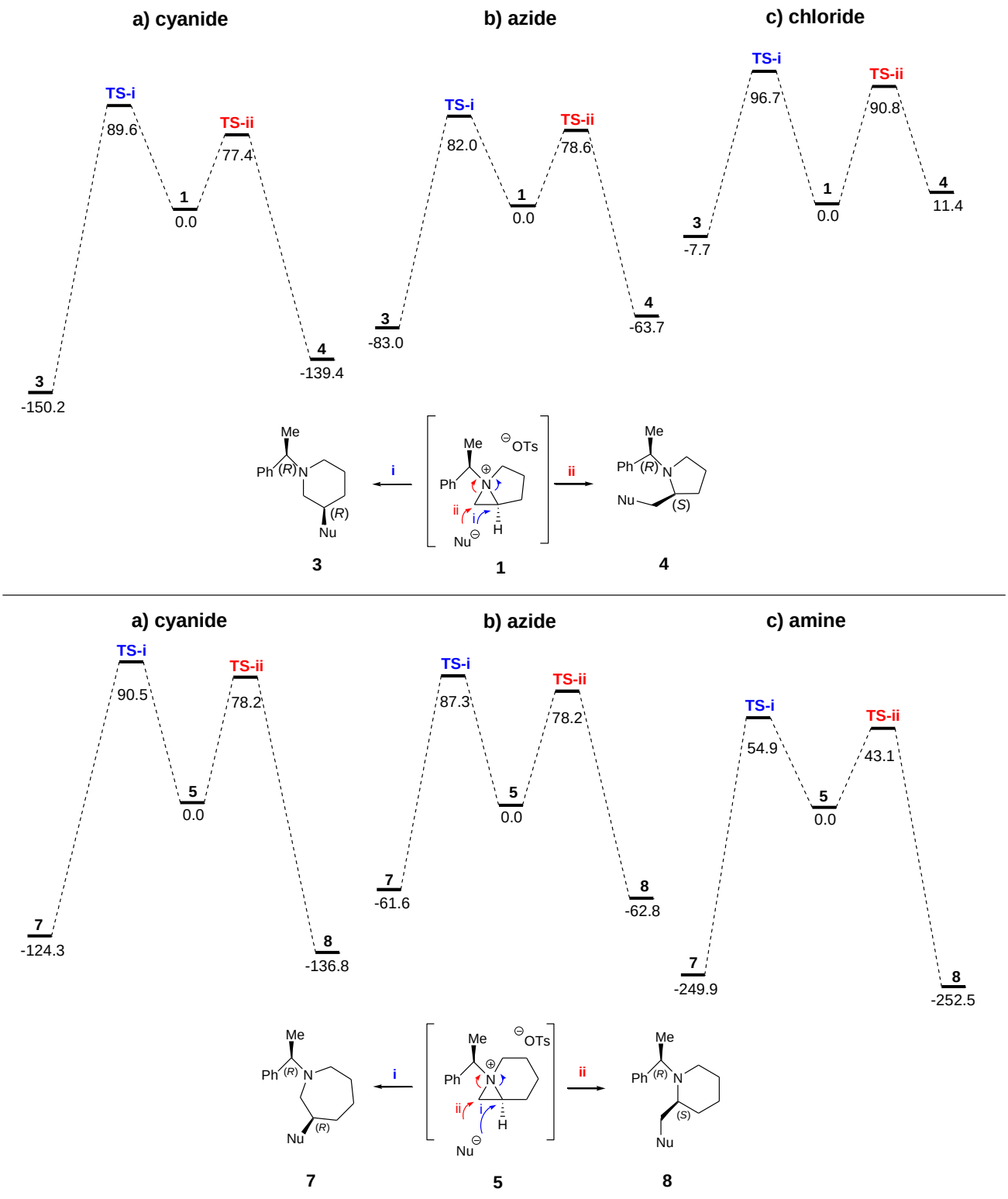

Figure 2. Gibbs free energy profiles for the ring-expansion of 1-azoniabicyclo[n.1.0]alkane **1** (top) and **5** (bottom) with different nucleophiles.

M06-2X/6-31+G(d,p), energies in kJ/mol at 298 K and 1 atm, IEFPCM in acetonitrile, (ε =35.688)

It is important to note that differences in barrier heights consistently show the same trend, regardless of level of theory or type of solvation employed. This brings confidence in the predictive power of the calculations and will be useful in future experimental studies on similar systems. At all levels of theory and levels of solvation, the thermodynamic product for the ring-opening of bicyclic aziridinium ion **1** is piperidine **3**, obtained *via* the hindered **path i**. Similarly, in the case of aziridinium **5**, piperidine **8**, obtained *via* the unhindered **path ii** is the thermodynamic product at all levels of theory and levels of solvation. Moreover, for both aziridinium ions **1** and **5**, the unhindered **path ii** is evidently the kinetically preferred route. Ultimately, the nucleophile's identity determines the experimental outcome, which in some cases yield the kinetic and in others the thermodynamic products. The free energy profiles (**Figure 2**) for each nucleophile reveal the rationale behind the experimentally observed outcomes.

Figure 2 shows the Gibbs free energy profiles for both systems, at the M06-2X/6-31+G(d,p) level of theory with IEFPCM solvation. The ring-expansion of aziridinium ion **1** with cyanide yields the kinetic product, pyrrolidines **4**. The rationale behind the unexpected experimental results is seen in the free energy profile in **Figure 2**. The kinetic product **4** is formed through the smaller free energy barrier (**path ii**, **TS-ii**), owing to the high reverse barriers (~217 kJ/mol), thermodynamic equilibration is not feasible, and cyanide exclusively affords the kinetic product **4**, despite piperidines **3** being the thermodynamic product. In the case of the chloride ion, although the kinetic product forms initially, consistent with experimental outcome, the ring-expansion eventually affords the thermodynamic product, piperidines **3**, due to low reverse barriers (~100 kJ/mol) that enable thermodynamic equilibration. Moreover, for the chloride nucleophile the difference in stability of products **3** and **4** is consistently in the order of 17 kJ/mol in favor of piperidine **3**, regardless of the level of theory. This is perfectly aligned with the experimental outcome (100:0

for **3**/**4**). For the azide nucleophile, free energy barriers for both pathways seem equally feasible, however, due to high reverse barriers, equilibration is not expected. This is in line with the experimentally observed product ratios (36:64 for **3**/**4**) for the azide induced ring-expansion of aziridiniums **1**.

In the nucleophile-induced ring-expansions of aziridinium ions **5**, some similarities to aziridinium ions **1** are observed, particularly for cyanide, there is a clear preference for the unhindered pathway (**path ii**) and the reaction yields piperidines **8**, in line with the experimentally observed regioselectivities (8:92 for **7**/**8**). Incidentally, piperidines **8** is also the thermodynamic product in all ring-expansions of aziridinium ions **5**, therefore thermodynamic equilibration, when reverse barriers are feasible, would still favor piperidines **8** over azepanes **7**. Free energy profiles for the ring-expansion of aziridiniums **5** with amines, depict very low barriers for both pathways (~50 kJ/mol) revealing the extremely reactive and, therefore, non-selective nature of the nucleophile. The barrier for the unhindered route (**path ii**) is ~10 kJ/mol lower, as expected; however, overall barrier heights are too low to expect a kinetic outcome at room temperature and both pathways are deemed feasible. Consistent with the experimental outcome (65:35 for **7**/**8**), both azepanes **7** and piperidines **8** are expected to form from the ring-expansion of aziridiniums **5** with amines. Additionally, ring-expansion of aziridinium **5** with metal amines show the highest exothermicity among all nucleophiles, hence, no thermal equilibration could be observed for these types of nucleophiles. These results indicate that although azepanes 7 are neither the kinetically nor thermodynamically favored product of aziridinium ion 5 ring-expansions, the formation of azepanes 7 is sufficiently feasible in the presence of very reactive nucleophiles, such as metal amines. In the case of the azide nucleophile, experimental results (59:41 for **7**/**8**) indicate a very slight preference for the formation of azepanes **7**. It is important to note that accurately reproducing

an experimental product ratio of 59:41 is not within the feasible accuracy level of current computational methods. However, the observed product ratios could be rationalized by studying the free energy profiles, where azepanes **7** and piperidines **8** are almost isoenergetic (-61.6 kJ/mol and -62.8 kJ/mol, respectively). Contrary to the amine case, where the reverse barriers were in the order of ~300 kJ/mol, for the azide, reverse barriers are shown to be more feasible, enabling thermodynamic equilibration.

Table 5. Gibbs free energies of activation ($\Delta G^{\ddagger}$) and reaction (ΔG_{rxn}) [kJ/mol] for the ring opening of bicyclic aziridinium ions **1** and **5** with different nucleophiles.[a,b]

		BMK/6-31+G(d,p)				MPW1K/6-31+G(d,p)				
		Path **i**	Path **ii**	Path **i**	Path **ii**	Path **i**	Path **ii**	Path **i**	Path **ii**	
	Nu	$\Delta G^{\ddagger}$		ΔG_{rxn}		$\Delta G^{\ddagger}$		ΔG_{rxn}		**Exp**[c]
1	**CN**	87.3	75.2	-140.1	-131.2	93.0	82.5	-155.4	-147.8	0:100
1	**N_3**	85.3	81.4	-70.5	-53.8	93.0	90.6	-74.2	-59.7	36:64
1	**Cl**	94.8	88.5	0.5	17.1	99.7	96.0	-0.93	14.9	100:0
5	**CN**	87.5	77.6	-116.2	-128.3	94.1	85.3	-129.8	-143.3	8:92
5	**N_3**	91.1	82.5	-51.6	-52.8	99.2	92.2	-54.5	-57.1	59:41
5	**NH_2**	54.8	46.4	-248.2	-252.0	63.1	52.1	-252.0	-256.7	65:35

[a] Single-point (IEFPCM ε =35.688) energies on M062X/6-31+G(d,p) IEFPCM (ε =35.688) optimized structures.
[b] All energies relative to the separate reactants.
[c] Experimental results **3:4** for aziridinium **1**, **7:8** for aziridinium **5.**

Computational findings were further extended by performing energy refinements (on both aziridinium systems with all nucleophiles) with kinetic functionals, BMK and MPW1K, well-known to give accurate barrier heights (**Table 5**).[27,50,62] Once again the formation of the kinetic product for the cyanide-induced ring-expansion of bicyclic aziridinium **1** is confirmed through unfeasibly high reverse barriers for thermodynamic equilibration. Azide displays similar preference for both attack sites in its reaction with aziridinium **1**, resulting in low regioselectivities. Ring-expansion products resulting from chloride attack on aziridinium **1** undergo thermal

equilibration to ultimately produce the thermodynamic product, piperidines **3**. The data resulting from kinetic functionals show that the barriers for amine-induced ring expansions of aziridinium **5** remain significantly lower than those for azide and cyanide, enabling the formation of both products. In the case of bicyclic aziridinium **5** with cyanide nucleophile, the kinetic route is shown to be favored, and piperidines **8**, which are also the thermodynamic products, are formed. For the azide case, similar product stabilities and feasible back barriers allowing thermal equilibration result in both regioisomers being formed.

Ring Distortion Energies

Previous studies regarding S_N2 reactions found that the central barrier of nucleophilic substitutions at an S_N2 type carbon is steric in nature, due to the pentavalent transition state.[63–65] This steric repulsion, which is destabilizing in nature, results in geometrical deformation, that requires a high distortion energy, ΔE_{dist}. In an effort to compare the difference in deformation caused by **path i** and **ii**, distortion energies were calculated for both aziridinium ions in their ring-expansion reactions with different nucleophiles, as shown in **Table 6**. For bicyclic aziridinium ion **1**, no clear distinction between the two paths is observed. However, distortion energies are shown to increase in the order of cyanide, azide and chloride, in line with bond elongation percentages discussed earlier. Moreover, the cost of distorting the bicyclic aziridinium ions and forming a reorganized structure corresponding to the transition state, is shown to increase as the nucleophile size increases. This is also consistent with experimental outcome, as seen in the case of chloride with aziridinium ion **1**, which has highly product-like transition states, in comparison to cyanide and azide. Distortion energies reported for bicyclic aziridinium ion **5** are also in agreement with their bond elongation percentages; while azide has the highest, NH_2^- has the lowest values for distortion, consistent with the very early nature of its transition state. There is a noteworthy difference

between distortion energies of path **i** and **ii** for cyanide attack to aziridinium ion **5**; attack on the less hindered carbon has less distortion, verifying the experimental outcome.

Table 6. Distortion energies for bicyclic aziridinium ions **1** and **5** in their ring-expansion reactions with different nucleophiles.

M06-2X/6-31+G(d,p) level of theory 298 K and 1 atm, IEFPCM in acetonitrile (ε =35.688).

		$\Delta E_{dist}^{\ddagger}$		$\Delta E_{int}^{\ddagger}$		
Nucleophile	Aziridinium	path **i**	path **ii**	path **i**	path **ii**	Exp[a]
CN^-	**1**	83.8	81.8	-32.3	-37.3	0:100
N_3^-	**1**	95.8	96.9	-52.0	-53.2	36:64
Cl^-	**1**	119.3	121.0	-49.1	-55.4	100:0
CN^-	**5**	98.1	88.7	-44.6	-48.5	8:92
N_3^-	**5**	103.7	102.8	-60.6	-64.5	59:41
NH_2^-	**5**	45.8	36.1	-33.3	-34.3	65:35

[a] Experimental results **3:4** for substrate **1**, **7:8** for substrate **5**.

CONCLUSION

Nucleophilic ring-expanison reactions of aziridinium ions **1** with cyanide, azide and chloride and aziridinium ions **5** with cyanide, azide and amine nucleophiles in acetonitrile have been investigated within a theoretical framework, to understand the underlying factors for the experimental outcomes and to guide experimental efforts towards higher regioselectivities by rationalizing the influence of the nucleophile and the bicyclic aziridinium's ring size. A thorough analysis of transition states was performed on both systems and both pathways, Gibbs free energy profiles were constructed with the inclusion of different solvation models as well as non-covalent interactions. Energetic analysis allowed for the identification of kinetic and thermodynamic routes, which were further reinforced by studying the nature of the transition state structures, the variations of critical bonds, as well as the effects of distortion.

In terms of computational methodologies employed, IEFPCM and CPCM optimizations yielded very similar results for each case. Activation barriers were shown to consistently increase with the M06-2X functional for each system, owing to the stabilization of the reactants. In the current study, the computed trends in regioselectivities were shown to be relatively robust across different levels of theory and the type of solvation method employed, allowing confident predictions through the calculated data. The thermodynamic product for bicyclic aziridinium ions **1** and **5** clearly appears to be piperidines **3** and piperidines **8**, respectively, at all levels of theory. For both aziridinium ions **1** and **5**, the unhindered **path ii** is shown to be the kinetically preferred route. However, the magnitude of the barrier heights for both pathways depends heavily on the nature of the nucleophile. Ultimately, a thorough investigation of the free energy profiles show that the nucleophile's identity determines the experimental outcome, which in some cases yield the kinetic and in others the thermodynamic products. Moreover, the current study helps predict ways in which the desired regioselective outcomes could be induced in future experimental studies on similar systems. Particularly, in the case of aziridinium ions **5**, ring-expansion products could be influenced by employing sterics on the bicyclic system and through careful selection of the nucleophile's character.

ACKNOWLEDGEMENTS

The numerical calculations reported in this paper were partially performed at the TUBITAK ULAKBIM, High Performance and Grid Computing Center (TRUBA resources) as well as the computational resources at CCBG (www.ccbg.chem.boun.edu.tr) funded by the Bogazici University Research Fund (BAP-SUP Project No. 8245).

REFERENCES

1 A. K. Yudin, in *Aziridines and Epoxides in Organic Synthesis*, ed. A. K. Yudin, Wiley-VCH Verlag GmbH & Co. KGaA, Weinheim, FRG, 2006, pp. 1–492.

2 M. K. Ghorai, A. Bhattacharyya, S. Das and N. Chauhan, in *Synthesis of 4- to 7-membered Heterocycles by Ring Expansion: Aza-, oxa- and thiaheterocyclic small-ring systems*, eds. M. D'hooghe and H.-J. Ha, Springer International Publishing, Cham, 2015, pp. 49–142.

3 B. Zwanenburg and P. ten Holte, in *Topics in Current Chemistry*, ed. P. Metz, Springer Berlin Heidelberg, Berlin, Heidelberg, 2001, vol. 216, pp. 93–124.

4 U. M. Lindström and P. Somfai, *Synthesis (Stuttg).*, 1998, **1998**, 109–117.

5 J. B. Sweeney, *Chem. Soc. Rev.*, 2002, **31**, 247–258.

6 X. E. Hu, *Tetrahedron*, 2004, 60, 2701–2743.

7 S. Stanković, M. D'hooghe, S. Catak, H. Eum, M. Waroquier, V. Van Speybroeck, N. De Kimpe and H.-J. Ha, *Chem. Soc. Rev.*, 2012, **41**, 643–665.

8 D. Tanner, *Angew. Chemie Int. Ed. English*, 1994, 33, 599–619.

9 C. Schjoeth-Eskesen, P. R. Hansen, A. Kjaer and N. Gillings, *ChemistryOpen*, 2015, **4**, 65–71.

10 A. Bhattacharyya, C. V Kavitha and M. K. Ghorai, *J. Org. Chem.*, 2016, **81**, 6433–6443.

11 H. Goossens, D. Hertsen, K. Mollet, S. Catak, M. D'hooghe, F. De Proft, P. Geerlings, N. De Kimpe, M. Waroquier and V. Van Speybroeck, in *Structure, Bonding and Reactivity of*

Heterocyclic Compounds, eds. F. De Proft and P. Geerlings, Springer Berlin Heidelberg, Berlin, Heidelberg, 2014, pp. 1–34.

12 T. Ohwada, H. Hirao and A. Ogawa, *J. Org. Chem.*, 2004, **69**, 7486–7494.

13 M. D'hooghe, K. Vervisch, A. Van Nieuwenhove and N. De Kimpe, *Tetrahedron Lett.*, 2007, **48**, 1771–1774.

14 H. Goossens, K. Vervisch, S. Catak, S. Stanković, M. D'Hooghe, F. De Proft, P. Geerlings, N. De Kimpe, M. Waroquier and V. Van Speybroeck, *J. Org. Chem.*, 2011, **76**, 8698–8709.

15 H. Eum, J. Choi, C.-G. Cho and H.-J. Ha, *Asian J. Org. Chem.*, 2015, **4**, 1399–1409.

16 A. Padwa, in *In Comprehensive Heterocyclic Chemistry III*, Elsevier, 2008, pp. 1–104.

17 H. S. Chong, H. A. Song, M. Dadwal, X. Sun, I. Sin and Y. Chen, *J. Org. Chem.*, 2010, **75**, 219–221.

18 T.-X. Métro, B. Duthion, D. Gomez Pardo and J. Cossy, *Chem. Soc. Rev.*, 2010, **39**, 89–102.

19 Y. Dong, H. Yun, C. S. Park, W. K. Lee and H. J. Ha, *Acta Crystallogr. Sect. C Cryst. Struct. Commun.*, 2003, **59**, 659–660.

20 Y. Kim, H.-J. Ha, S. Y. Yun and W. K. Lee, *Chem. Commun.*, 2008, **0**, 4363–4365.

21 M. D'hooghe, V. Van Speybroeck, M. Waroquier and N. De Kimpe, *Chem. Commun. (Camb).*, 2006, **0**, 1554–1556.

22 B. Anxionnat, B. Robert, P. George, G. Ricci, M. A. Perrin, D. Gomez Pardo and J.

Cossy, *J. Org. Chem.*, 2012, **77**, 6087–6099.

23 M. Nonn, A. M. Remete, F. Fülöp and L. Kiss, *Tetrahedron*, 2017, 73, 5461–5483.

24 J. Dolfen, N. N. Yadav, N. De Kimpe, M. D'hooghe and H. J. Ha, *Adv. Synth. Catal.*, 2016, 358, 3485–3511.

25 M. K. Ji, D. Hertsen, D. H. Yoon, H. Eum, H. Goossens, M. Waroquier, V. Vanspeybroeck, M. D'Hooghe, N. Dekimpe and H. J. Ha, *Chem. - An Asian J.*, 2014, **9**, 1060–1067.

26 J. Choi, N. N. Yadav and H. J. Ha, *Asian J. Org. Chem.*, 2017, **6**, 1292–1307.

27 S. Catak, M. D'Hooghe, N. De Kimpe, M. Waroquier and V. Van Speybroeck, *J. Org. Chem.*, 2010, **75**, 885–896.

28 Y. Lam, M. N. Grayson, M. C. Holland, A. Simon and K. N. Houk, *Acc. Chem. Res.*, 2016, **49**, 750–762.

29 L. A. Burns, Á. V.- Mayagoitia, B. G. Sumpter and C. D. Sherrill, *J. Chem. Phys.*, 2011, **134**, 84107.

30 N. Marom, A. Tkatchenko, M. Rossi, V. V. Gobre, O. Hod, M. Scheffler and L. Kronik, *J. Chem. Theory Comput.*, 2011, **7**, 3944–3951.

31 G. A. Dilabio and A. Otero-de-la-Roza, in *Reviews in Computational Chemistry*, 2016, vol. 29, pp. 1–97.

32 A. Becke, *J. Chem. Phys.*, 1993, **98**, 5648–5652.

33 Y. Zhao and D. G. Truhlar, *Theor. Chem. Acc.*, 2008, **120**, 215–241.

34 S. Grimme, *J. Comput. Chem.*, 2006, **27**, 1787–1799.

35 S. Grimme, J. Antony, S. Ehrlich and H. Krieg, *J. Chem. Phys.*, 2010, **132**, 154104.

36 B. J. Lynch, P. L. Fast, M. Harris and D. G. Truhlar, *J. Phys. Chem. A*, 2000, **104**, 4811–4815.

37 A. D. Boese and J. M. L. Martin, *J. Chem. Phys.*, 2004, **121**, 3405–3416.

38 J. R. C. M.J. Frisch, G.W. Trucks, H.B. Schlegel, G.E. Scuseria, M.A. Robb, M. C. G. Scalmani, V. Barone, B. Mennucci, G.A. Petersson, H. Nakatsuji, M. X. Li, H.P. Hratchian, A.F. Izmaylov, J. Bloino, G. Zheng, J.L. Sonnenberg, Y. Hada, M. Ehara, K. Toyota, R. Fukuda, J. Hasegawa, M. Ishida, T. Nakajima, F. O. Honda, O. Kitao, H. Nakai, T. Vreven, J.J.A. Montgomery, J.E. Peralta, R. M. Bearpark, J.J. Heyd, E. Brothers, K.N. Kudin, V.N. Staroverov, T. Keith, J. Kobayashi, J. Normand, K. Raghavachari, A. Rendell, J.C. Burant, S.S. Iyengar, V. B. Tomasi, M. Cossi, N. Rega, J.M. Millam, M. Klene, J.E. Knox, J.B. Cross, R. C. Adamo, J. Jaramillo, R. Gomperts, R.E. Stratmann, O. Yazyev, A.J. Austin, V. G. Z. Cammi, C. Pomelli, J.W. Ochterski, R.L. Martin, K. Morokuma, J. B. G.A. Voth, P. Salvador, J.J. Dannenberg, S. Dapprich, A.D. Daniels, O. Farkas and D. J. F. Foresman, J.V. Ortiz, J. Cioslowski, *Gaussian 09 Revis. E.01*, 2010.

39 C. Gonzalez and H. B. Schlegel, *J. Chem. Phys.*, 1989, **90**, 2154–2161.

40 C. Gonzalez and H. B. Schlegel, *J. Phys. Chem*, 1990, **94**, 5523–5527.

41 M. D'Hooghe, V. Van Speybroeck, A. Van Nieuwenhove, M. Waroquier and N. De Kimpe, *J. Org. Chem.*, 2007, **72**, 4733–4740.

42 S. Stanković, H. Goossens, S. Catak, M. Tezcan, M. Waroquier, V. Van Speybroeck, M. D'Hooghe and N. De Kimpe, *J. Org. Chem.*, 2012, **77**, 3181–3190.

43 V. Barone and M. Cossi, *J. Phys. Chem. A*, 1998, **102**, 1995–2001.

44 B. Mennucci, *Wiley Interdiscip. Rev. Comput. Mol. Sci.*, 2012, 2, 386–404.

45 A. Klamt, C. Moya and J. Palomar, *J. Chem. Theory Comput.*, 2015, **11**, 4220–4225.

46 Y. Takano and K. N. Houk, *J. Chem. Theory Comput.*, 2005, **1**, 70–77.

47 S. Catak, M. Dhooghe, T. Verstraelen, K. Hemelsoet, A. Van Nieuwenhove, H. J. Ha, M. Waroquier, N. De Kimpe and V. Van Speybroeck, *J. Org. Chem.*, 2010, **75**, 4530–4541.

48 M. D'Hooghe, S. Catak, S. Stankovic, M. Waroquier, Y. Kim, H. J. Ha, V. Van Speybroeck and N. De Kimpe, *European J. Org. Chem.*, 2010, **2**, 4920–4931.

49 S. Stanković, S. Catak, M. D'Hooghe, H. Goossens, K. Abbaspour Tehrani, P. Bogaert, M. Waroquier, V. Van Speybroeck and N. De Kimpe, *J. Org. Chem.*, 2011, **76**, 2157–2167.

50 L. Hermosilla, S. Catak, V. Van Speybroeck, M. Waroquier, J. Vandenbergh, F. Motmans, P. Adriaensens, L. Lutsen, T. Cleij and D. Vanderzande, *Macromolecules*, 2010, **43**, 7424–7433.

51 C. P. Kelly, C. J. Cramer and D. G. Truhlar, *J. Phys. Chem. A*, 2006, **110**, 2493–2499.

52 J. R. Pliego and J. M. Riveros, *J. Phys. Chem. A*, 2001, **105**, 7241–7247.

53 E. F. Da Silva, H. F. Svendsen and K. M. Merz, *J. Phys. Chem. A*, 2009, **113**, 6404–6409.

54 W.-J. van Zeist and F. M. Bickelhaupt, *Org. Biomol. Chem.*, 2010, **8**, 3118.

55 I. Fernández and F. M. Bickelhaupt, *Chem. Soc. Rev.*, 2014, **43**, 4953–4967.

56 F. M. Bickelhaupt and K. N. Houk, *Analyzing Reaction Rates with the Distortion/Interaction-Activation Strain Model*, 2017, vol. 56.

57 S. Agopcan, N. Çelebi-Ölçüm, M. N. Üçışık, A. Sanyal and V. Aviyente, *Org. Biomol. Chem.*, 2011, **9**, 8079–88.

58 A. G. Green, P. Liu, C. A. Merlic and K. N. Houk, *J. Am. Chem. Soc.*, 2014, **136**, 4575–4583.

59 S. M. Bronner, J. L. MacKey, K. N. Houk and N. K. Garg, *J. Am. Chem. Soc.*, 2012, **134**, 13966–13969.

60 F. Liu, R. S. Paton, S. Kim, Y. Liang and K. N. Houk, *J. Am. Chem. Soc.*, 2013, **135**, 15642–15649.

61 M. Walker, A. J. A. Harvey, A. Sen and C. E. H. Dessent, *J. Phys. Chem. A*, 2013, **117**, 12590–12600.

62 J. Dolfen, E. B. Boydas, V. Van Speybroeck, S. Catak, K. Van Hecke and M. D'hooghe, *J. Org. Chem.*, 2017, **82**, 10092–10109.

63 M. A. Van Bochove, M. Swart and F. M. Bickelhaupt, *ChemPhysChem*, 2007, **8**, 2452–2463.

64 A. P. Bento and F. M. Bickelhaupt, *J. Org. Chem.*, 2007, **72**, 2201–2207.

65 A. P. Bento and F. M. Bickelhaupt, *Chem. - An Asian J.*, 2008, **3**, 1783–1792.